

SUPPORTING INFORMATION

From Benzodithiophene to Diethoxy- Benzodithiophene Covalent Organic Frameworks - Structural Investigations

Maria S. Lohse^{a†}, Julian M. Rotter^{a†}, Johannes T. Margraf^b, Veronika Werner^a, Matthias Becker^a,
Simon Herbert^a, Paul Knochel^a, Timothy Clark^b, Thomas Bein^{a,*} and Dana D. Medina^{a,*}

^aDepartment of Chemistry and Center for NanoScience (CeNS), University of Munich (LMU), Butenandtstr. 5-13, 81377 Munich, Germany

^bFriedrich-Alexander-University Erlangen-Nürnberg (FAU), Computer-Chemie-Centrum, Nögelsbachstraße 25, 91052 Erlangen, Germany

Table of Contents

Section 1.	BDT-OEt COF simulated structures	2
Section 2.	Molecular dynamics simulations	11
Section 3.	Nitrogen sorption.....	12
Section 4.	SEM micrographs.....	13
Section 5.	TEM micrographs.....	14
Section 6.	Thermogravimetric analysis	15
Section 7.	FT-IR spectra.....	18
Section 8.	PXRD small angle region	19
Section 9.	Solid state NMR spectra of BDT-OEt COF	20
Section 10.	NMR spectra of hydrolysed COFs	21

Section 1. BDT-OEt COF simulated structures

Molecular mechanics simulations for the BDT-OEt COF unit cell were carried out using Materials Studio software 4.4 and the Forcite module. First, we constructed a bare hexagonal $P6$ space group unit cell with lattice parameters reported for the BDT-COF. Based on the functional groups and the geometry of the BDT-OEt COF precursor molecules, the repeating unit was constructed and placed in the bare hexagonal unit cell to obtain the complete unit cell. The geometry of the BDT-OEt COF layer was optimized in the unit cell using the Dreiding forcefield and the QEq correction for weak interactions. The Reflex package in the Materials Studio software allows for Pawley refinement for the simulated unit cell parameters according to the experimental PXRD. The simulated unit cell parameters were refined against the experimental PXRD. The refinement parameters R_p and R_{wp} are 3.37% and 4.95%, respectively, the final unit cell parameters are $a = b = 36.56 \pm 0.04 \text{ \AA}$, $c = 3.65 \pm 0.04 \text{ \AA}$.

Table S1. Refined crystal data.

Formula	$C_{78} O_{18} B_6 S_6 H_{48}$
Formula weight	1530.49 g/mol
Crystal system	Hexagonal
Space group	$P6$
Unit cell dimensions	$a = b = 36.56 \text{ \AA}$ $c = 3.65 \text{ \AA}$
Cell Volume	4234.14 \AA^3

Table S2. Fractional atomic coordinates.

Atom	Wyck.	x	y	z
C1	6d	0.58577	0.36594	0.44433
C2	6d	0.58777	0.32954	0.44062
C3	6d	0.49211	0.45890	0.47547
C4	6d	0.56198	0.47912	0.46663
C5	6d	0.54195	0.53395	0.48791
C6	6d	0.66044	0.40711	0.44743
C7	6d	0.62166	0.40426	0.44828
O8	6d	0.55181	0.37005	0.44579
B9	6d	0.56817	0.41435	0.45221
O10	6d	0.61299	0.43536	0.45323
C11	6d	0.54370	0.43609	0.45827
C12	6d	0.53300	0.49234	0.47430
S13	6d	0.48972	0.41092	0.45743
C14	6d	0.66425	0.37067	0.44362
C15	6d	0.62683	0.33073	0.44244
H16	6d	0.55974	0.30310	0.43696
H17	6d	0.59341	0.49907	0.46773
H18	6d	0.68480	0.43656	0.45058
O19	6d	0.58285	0.56389	0.51939
C20	6d	0.60015	0.60358	0.69692
C21	6d	0.64333	0.61313	0.83124
H22	6d	0.58033	0.60202	0.92893
H23	6d	0.60269	0.62792	0.50983
H24	6d	0.66339	0.61603	0.59942
H25	6d	0.63977	0.58737	1.00418
H26	6d	0.65821	0.64193	0.99045

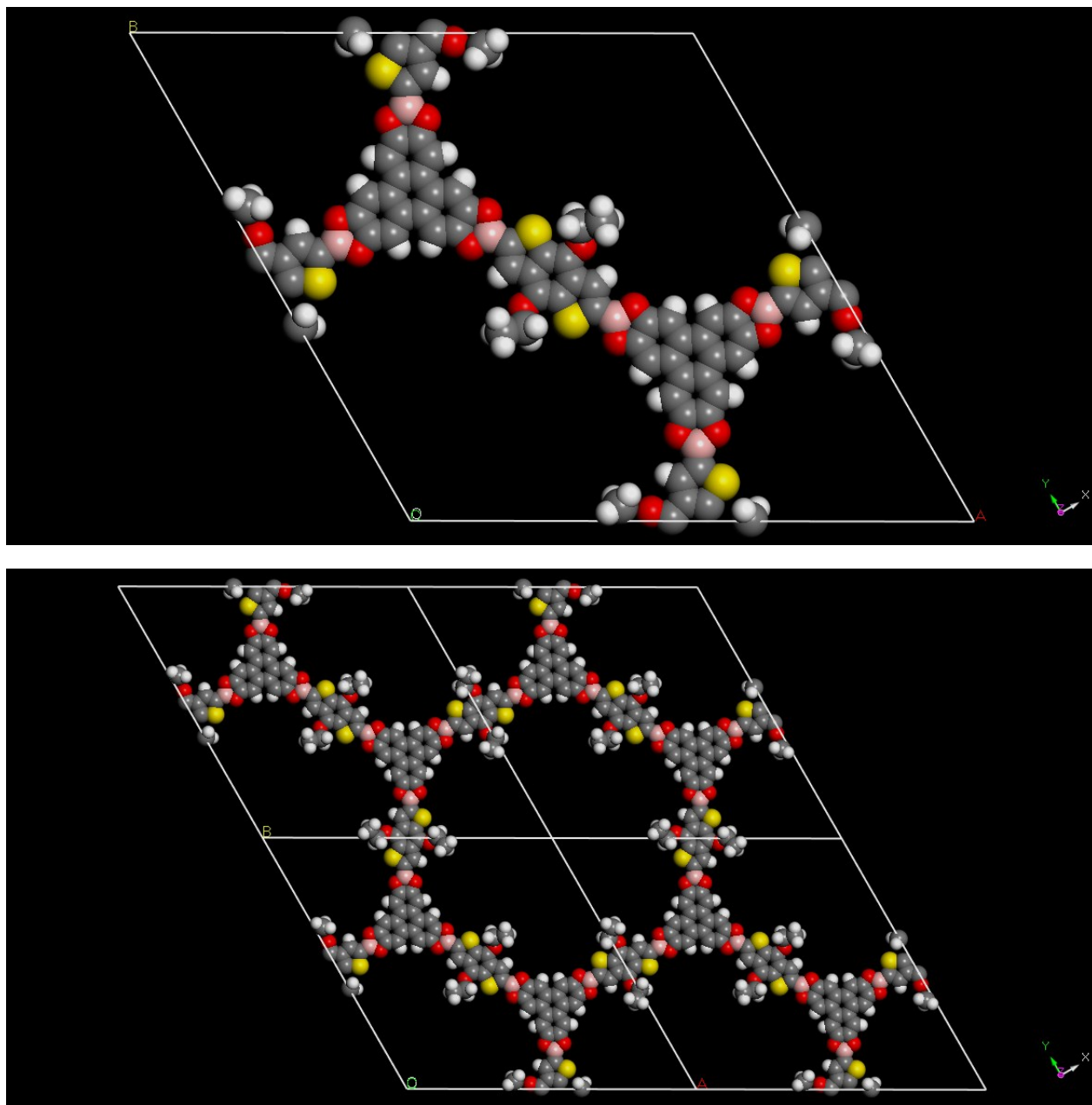


Figure S1. Simulation of BDT-OEt COF unit cells calculated in an eclipsed arrangement in the $P6$ space group. **Top:** top view on ab plane, **bottom:** four BDT-OEt COF unit cells fused to form the hexagonal pore.

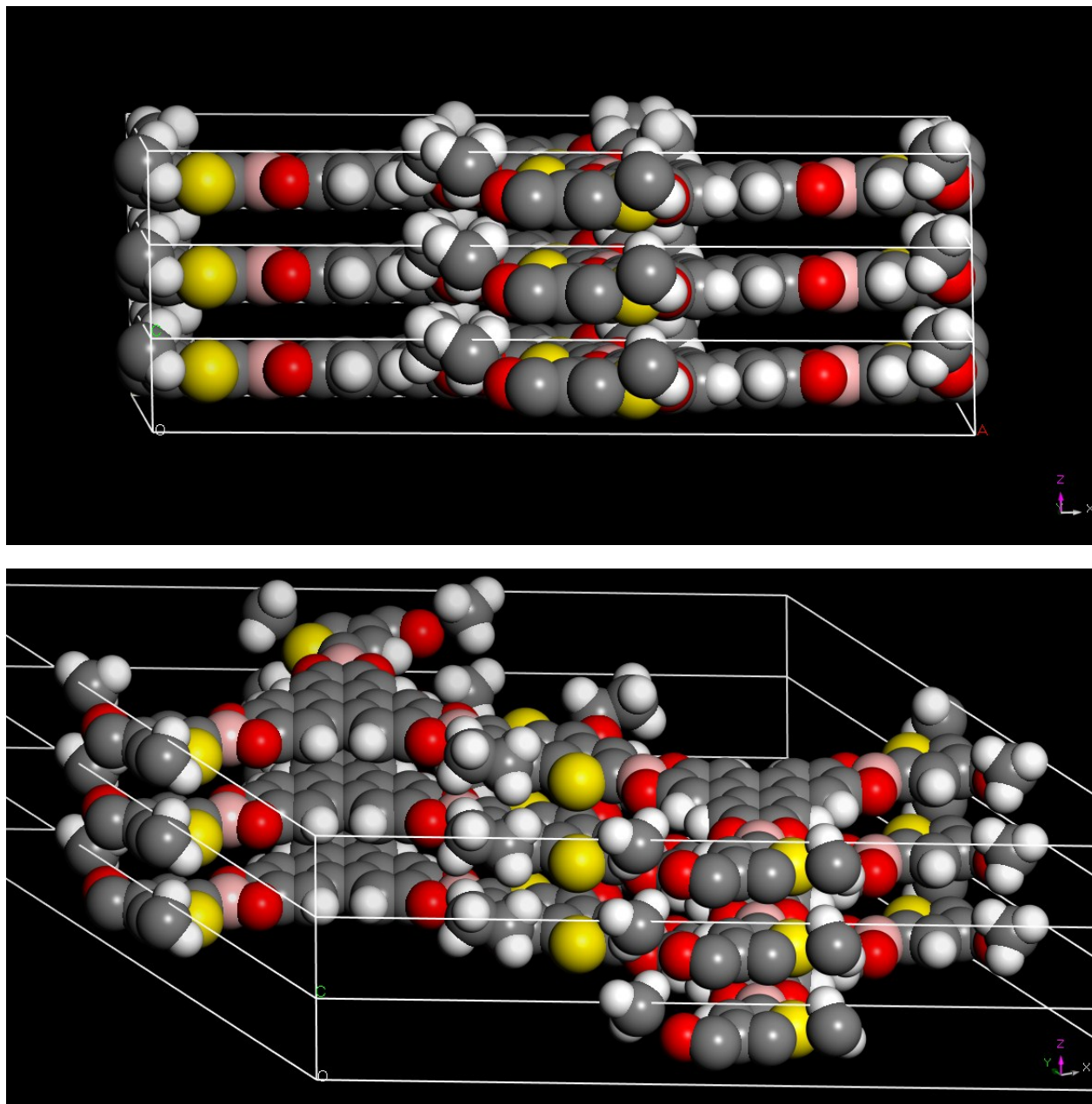


Figure S2. Simulation of BDT-OEt COF unit cell in an eclipsed arrangement in the $P6$ space group viewed along the c-axis with an interlayer distance of 3.65 Å.

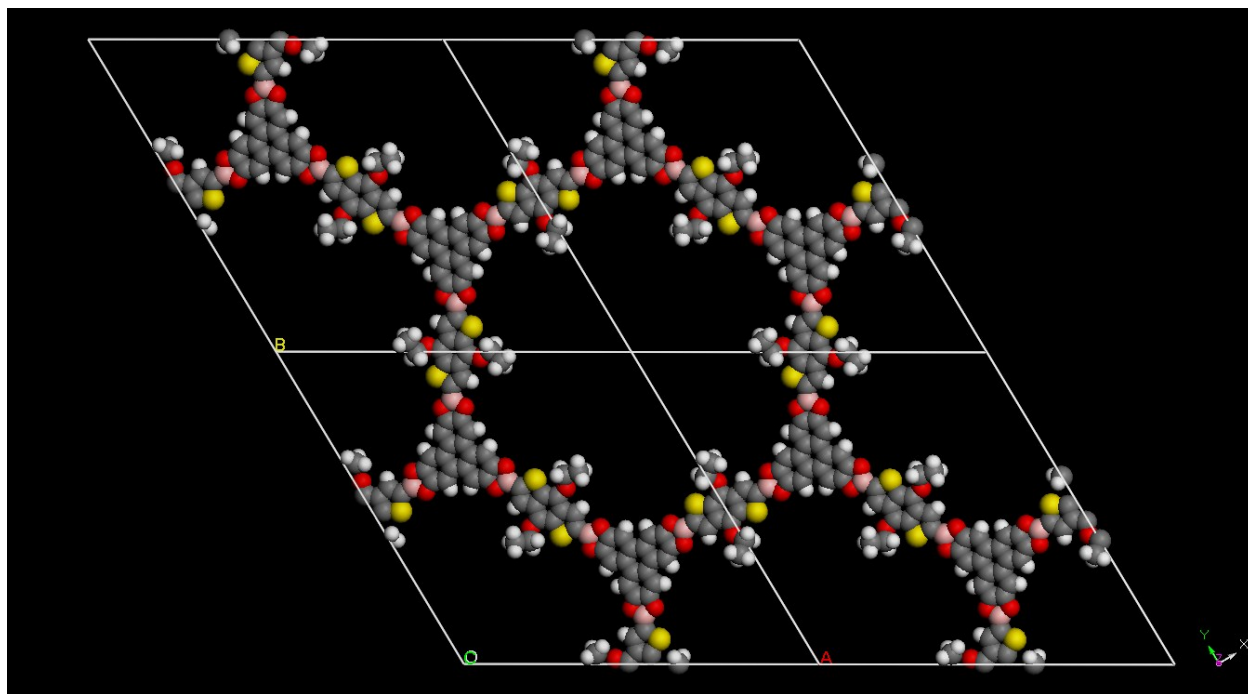
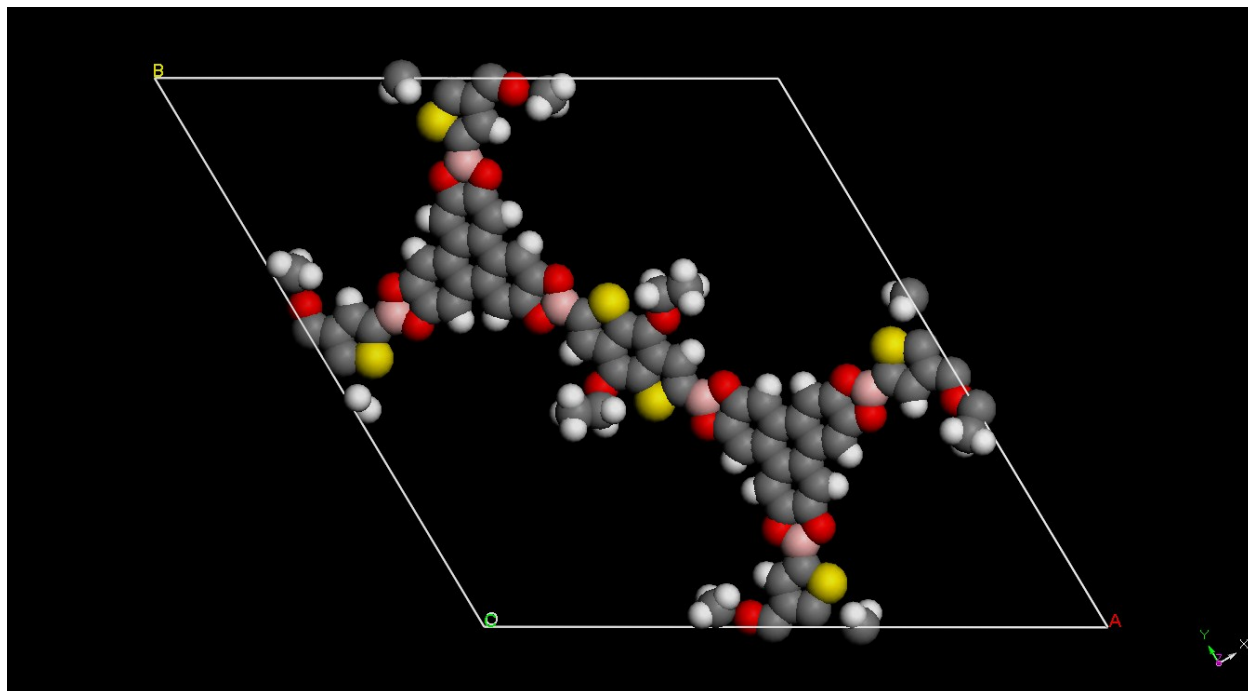


Figure S3. Simulation of BDT-OEt COF unit cells calculated in an eclipsed arrangement in the $P1$ space group. **Top:** top view on ab plane, **bottom:** four BDT-OEt COF unit cells fused to form the hexagonal pore.

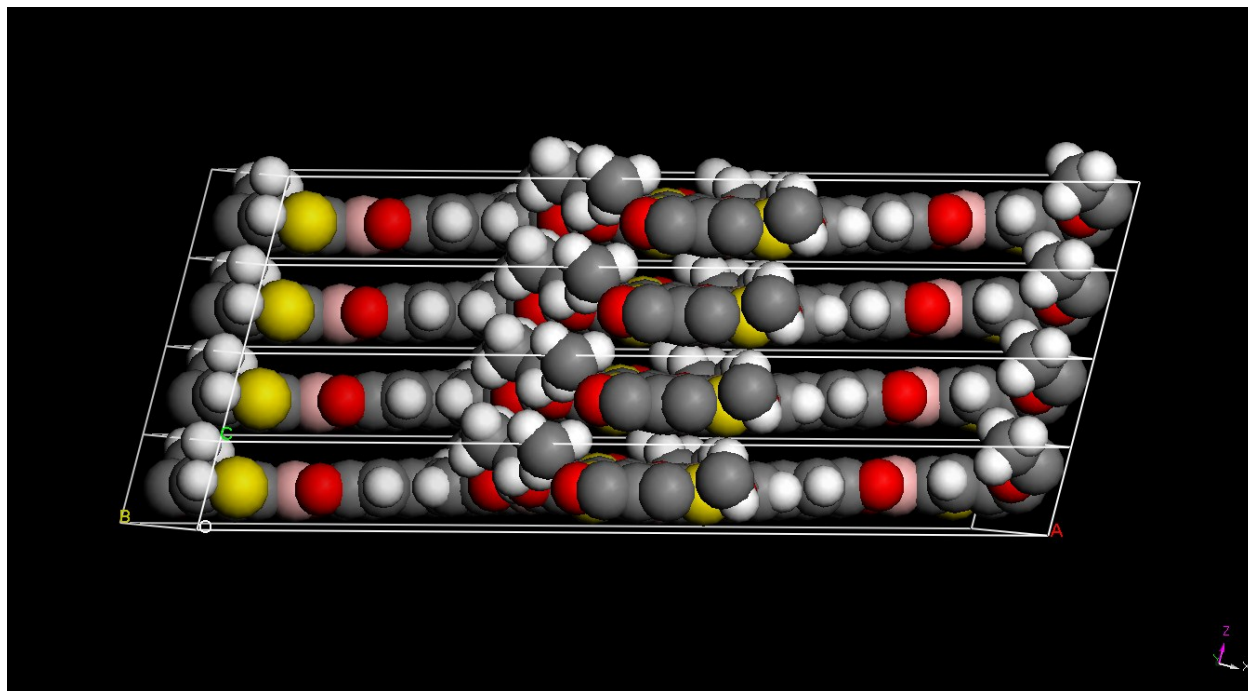


Figure S4. Simulation of the BDT-OEt COF unit cell in the $P1$ space group viewed along the c -axis.

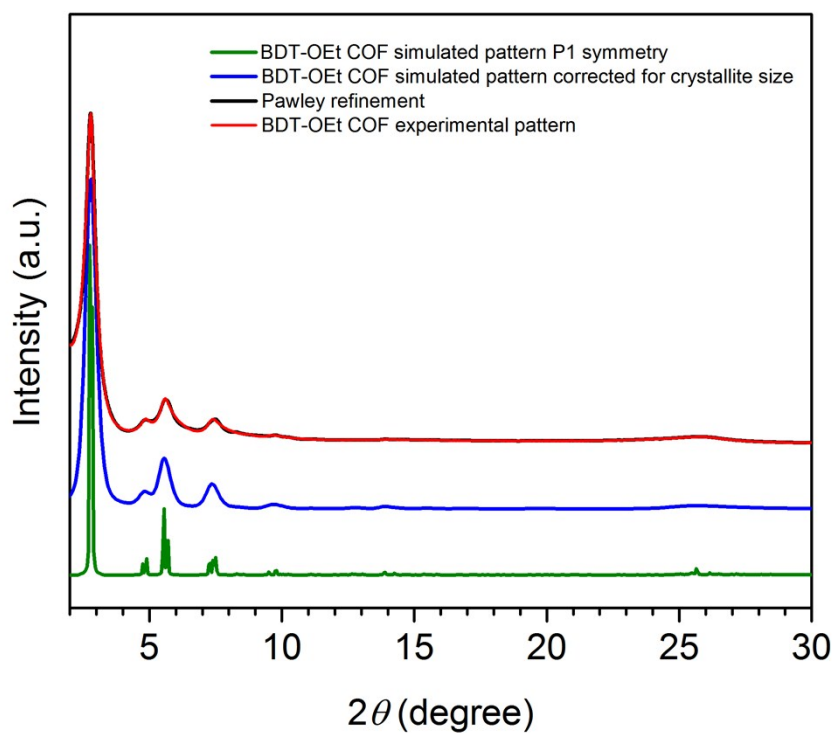


Figure S5. XRD patterns of BDT-OEt COF in $P1$ space group: experimental (red), Pawley refinement (black), simulated pattern corrected for crystallite size (blue), and simulated pattern (green). For Pawley refinement: The refinement parameters R_p and R_{wp} are 2.87% and 2.16%, respectively, the refined unit cell parameters are $a = 37.15 \text{ \AA} \pm 0.04$, $b = 37.17 \text{ \AA} \pm 0.04$, $c = 3.58 \pm 0.04 \text{ \AA}$; $\alpha = 90.31^\circ$, $\beta = 77.44^\circ$, $\gamma = 120.35^\circ$.

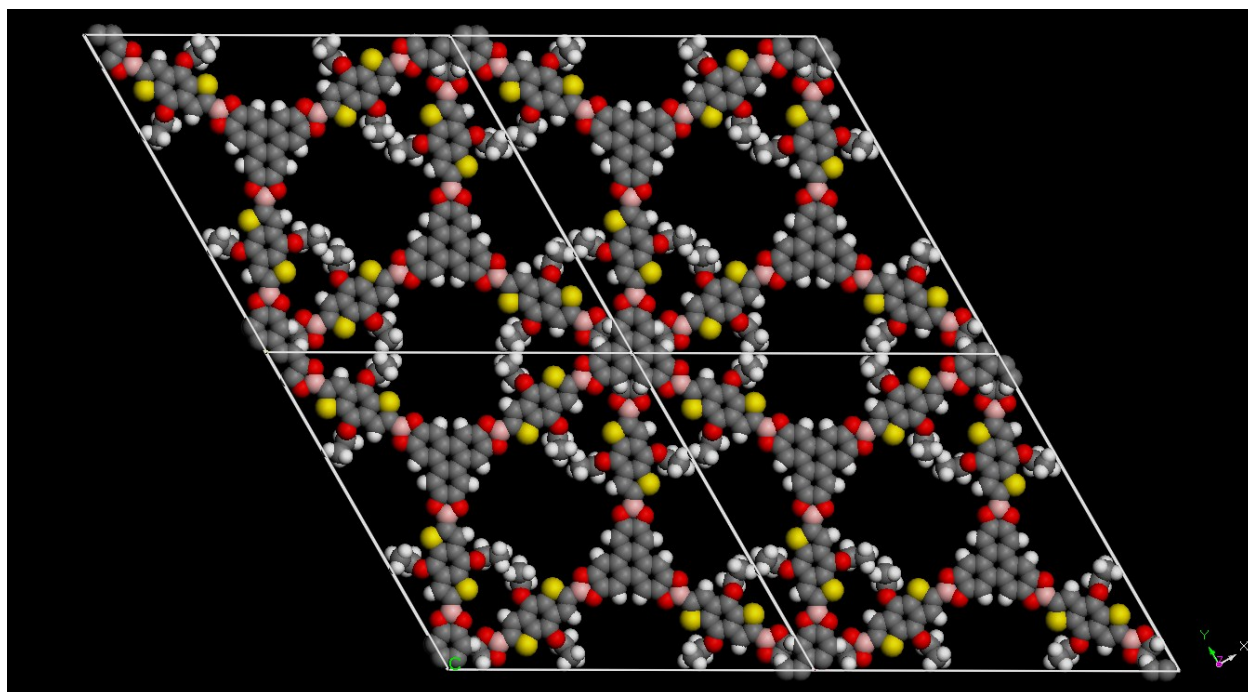
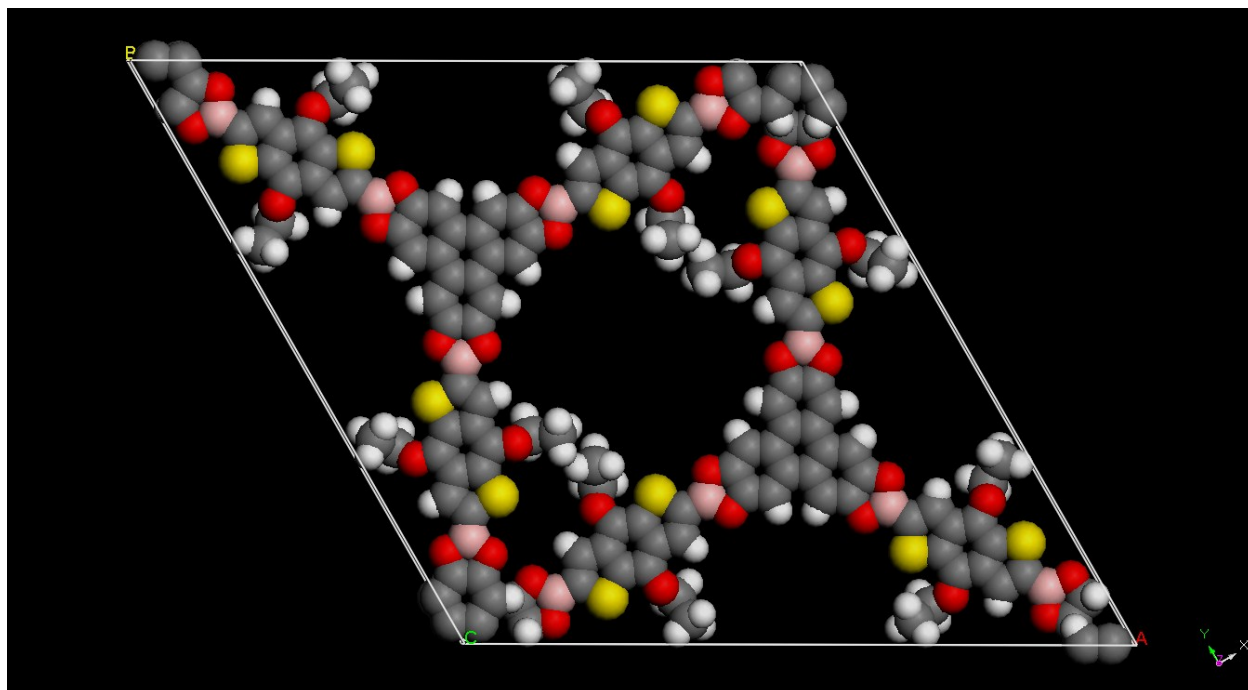


Figure S6. Simulation of BDT-OEt COF unit cells calculated in a staggered arrangement with $P6_3$ space group. **Top:** top view on ab plane, **bottom** four BDT-OEt COF unit cells fused to form the pore system.

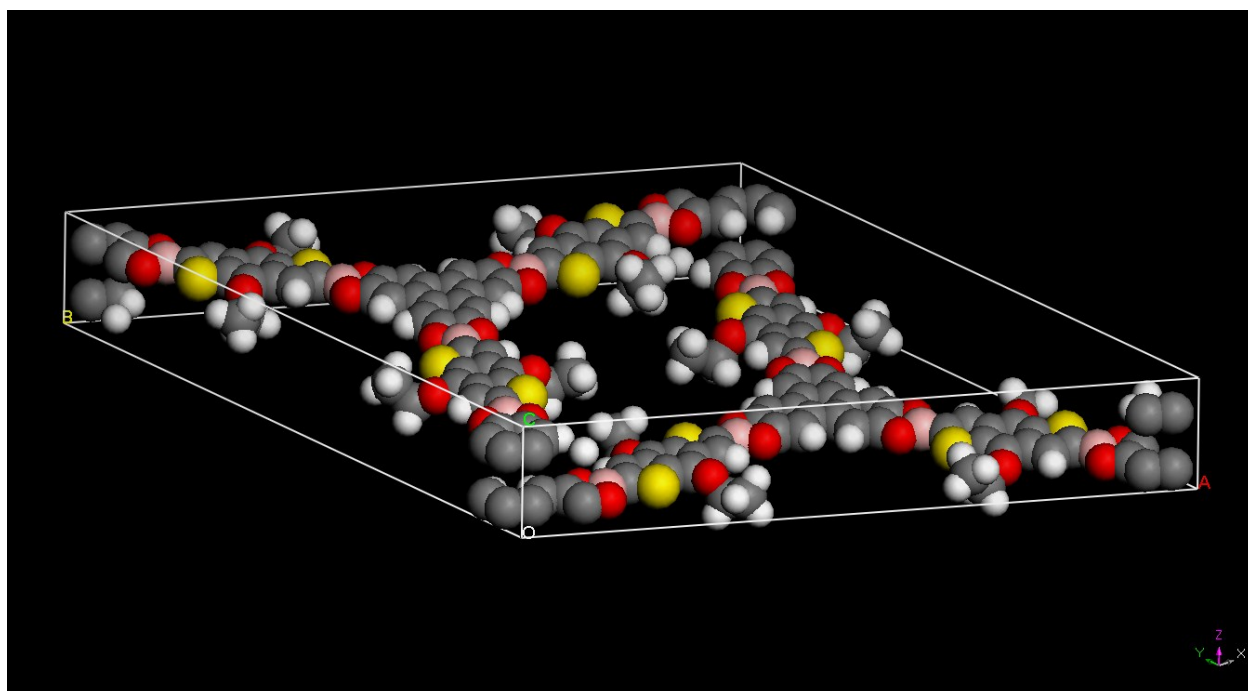
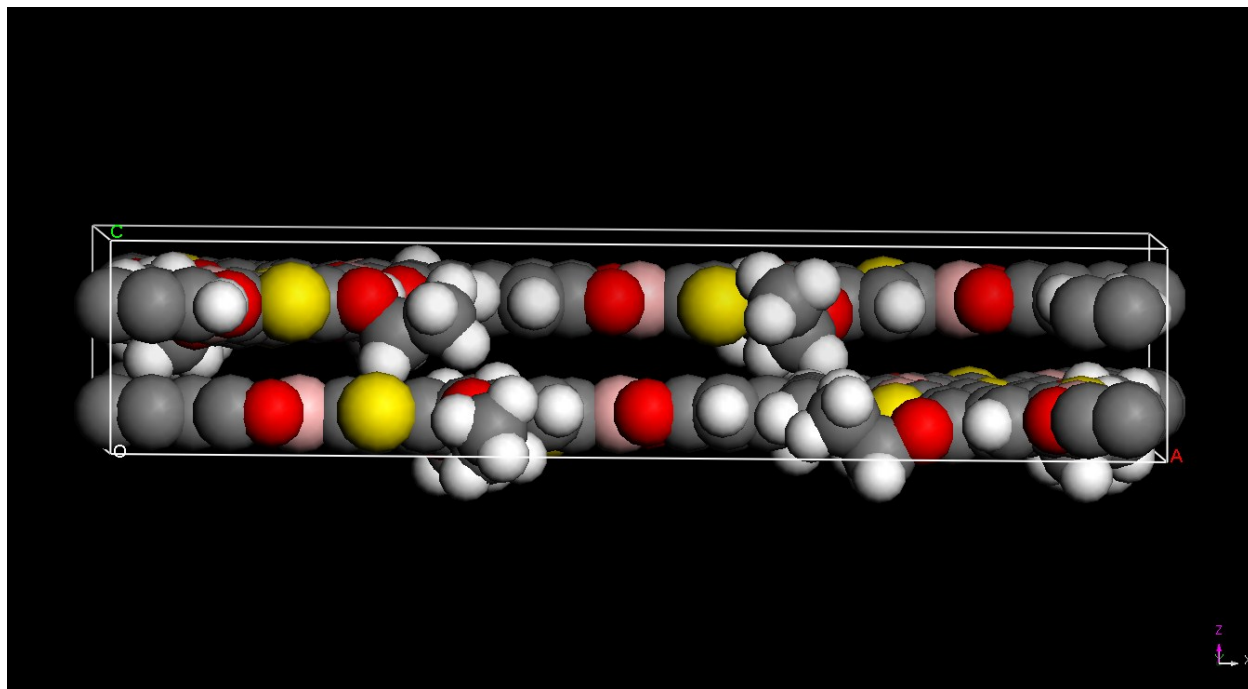


Figure S7. Simulation of the BDT-OEt COF unit cell in a staggered arrangement, viewed along the c-axis.

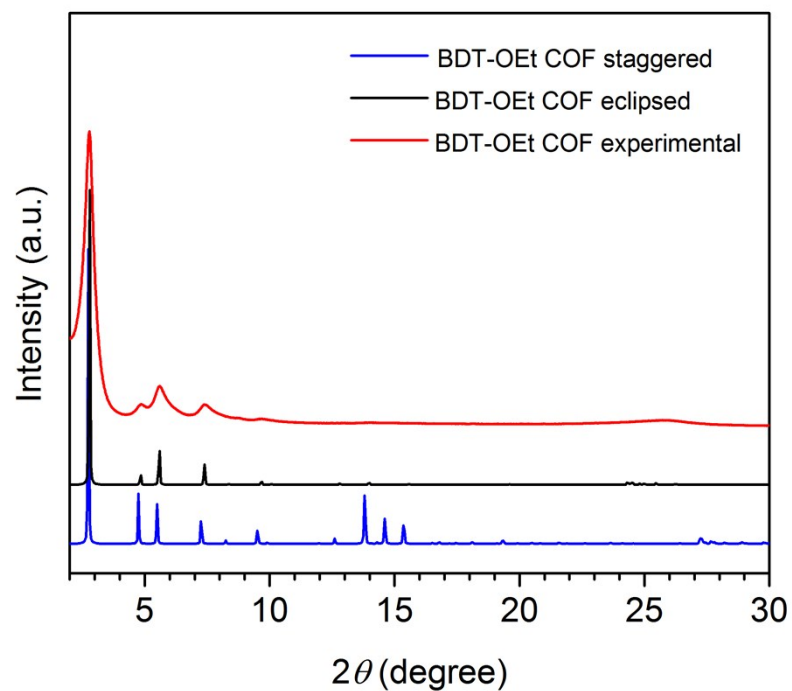


Figure S8. XRD patterns of BDT-OEt COF: experimental (red), simulated AA eclipsed arrangement (black), and simulated AB staggered arrangement (blue).

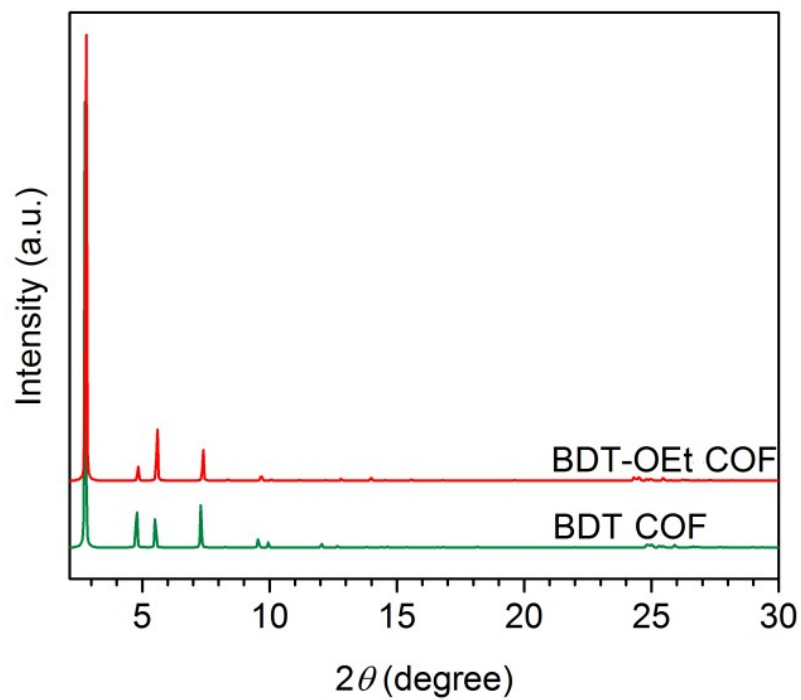


Figure S9. Comparison of simulated XRD patterns of BDT COF (green) and BDT-OEt COF (red).

Section 2. Molecular dynamics simulations

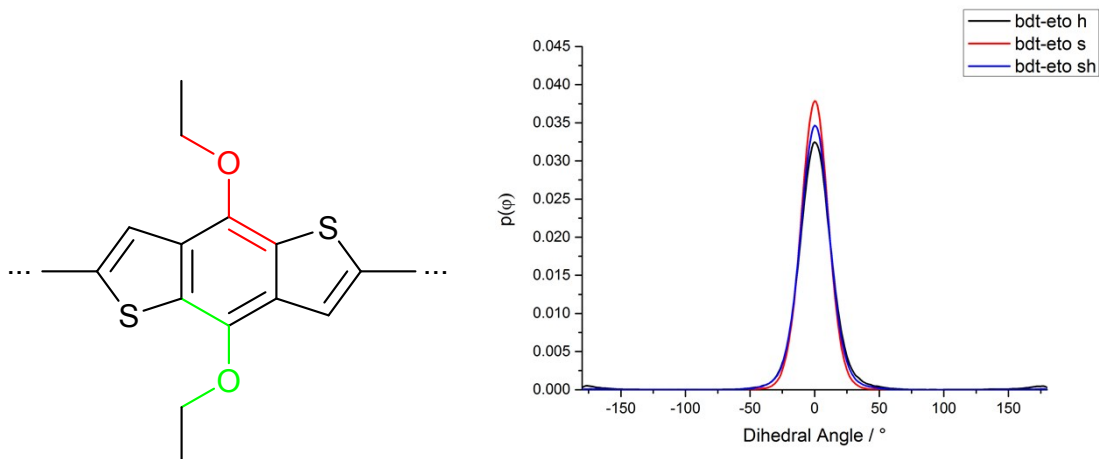


Figure S10. Left: Molecular structure of the ethoxy-substituted BDT unit. The possible initial orientations for the dihedral angle are shown in red (facing hydrogen, 180°) and green (facing sulfur, 0°). Right: Probability distribution of the dihedral angle sampled over 10 ns. Almost all dihedrals reorient to face the sulfur atom within the equilibration period of 0.1 ns, independent of the starting orientation (s = sulfur, h = hydrogen, sh = mixed).

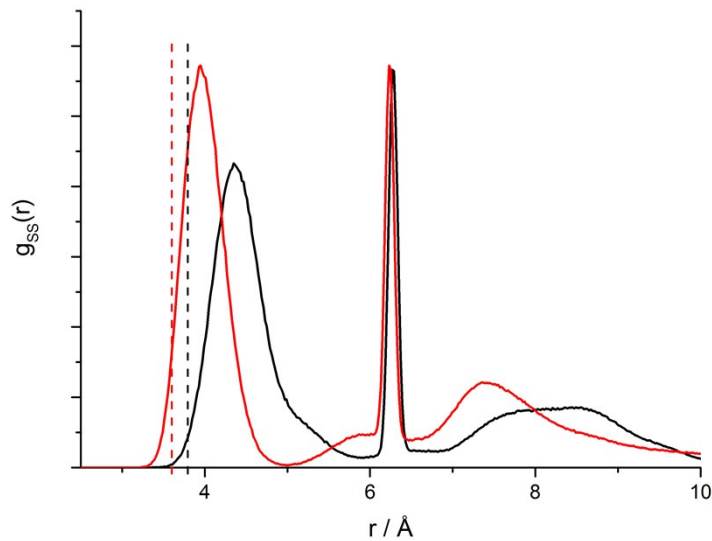


Figure S11. Sulfur-sulfur radial distribution functions of the ethoxy substituted (black) and pristine (red) BDT-COF. The vertical, dotted lines indicate the respective average interlayer distance.

Section 3. Nitrogen sorption

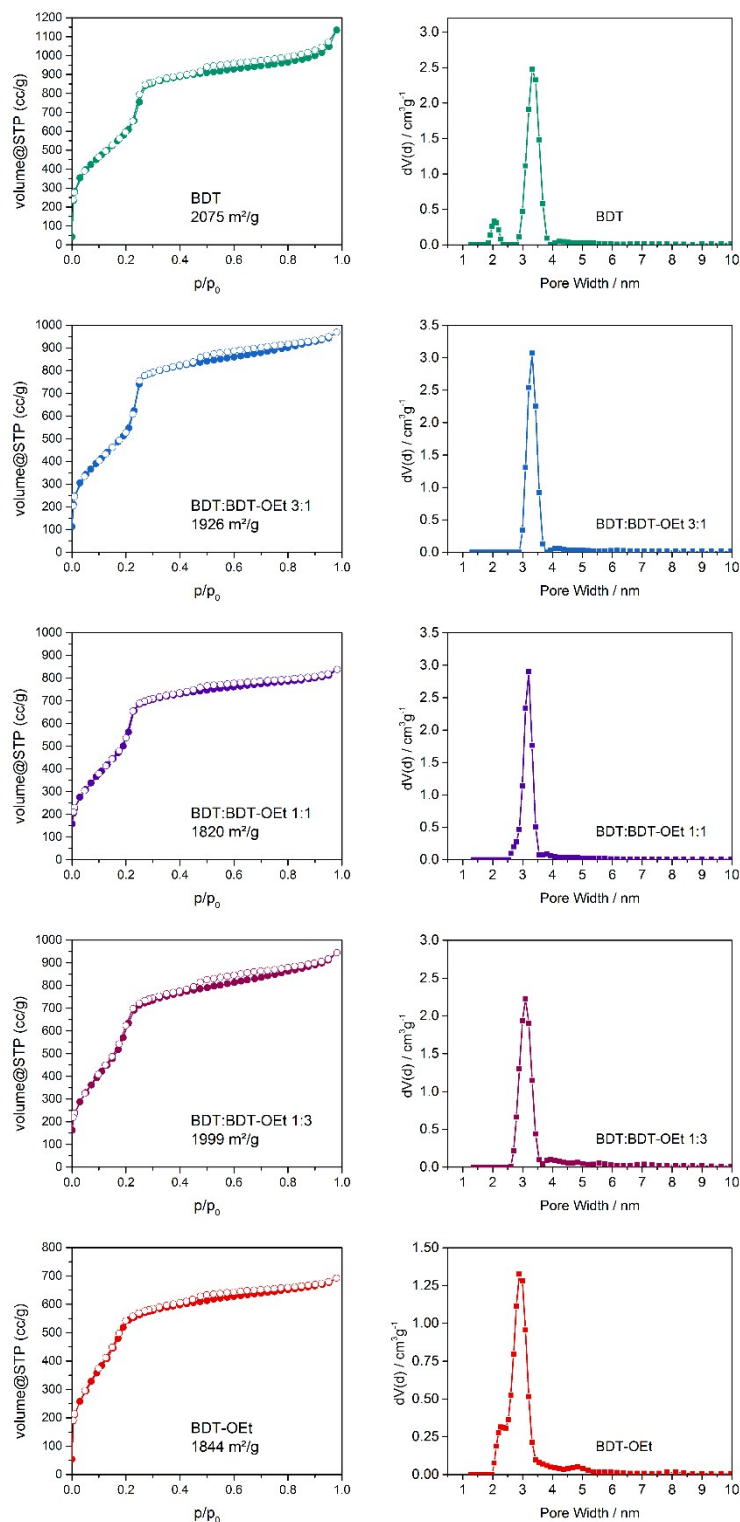


Figure S12. Nitrogen sorption isotherms of the COF powders (left) and pore size distributions (right).

Section 4. SEM micrographs

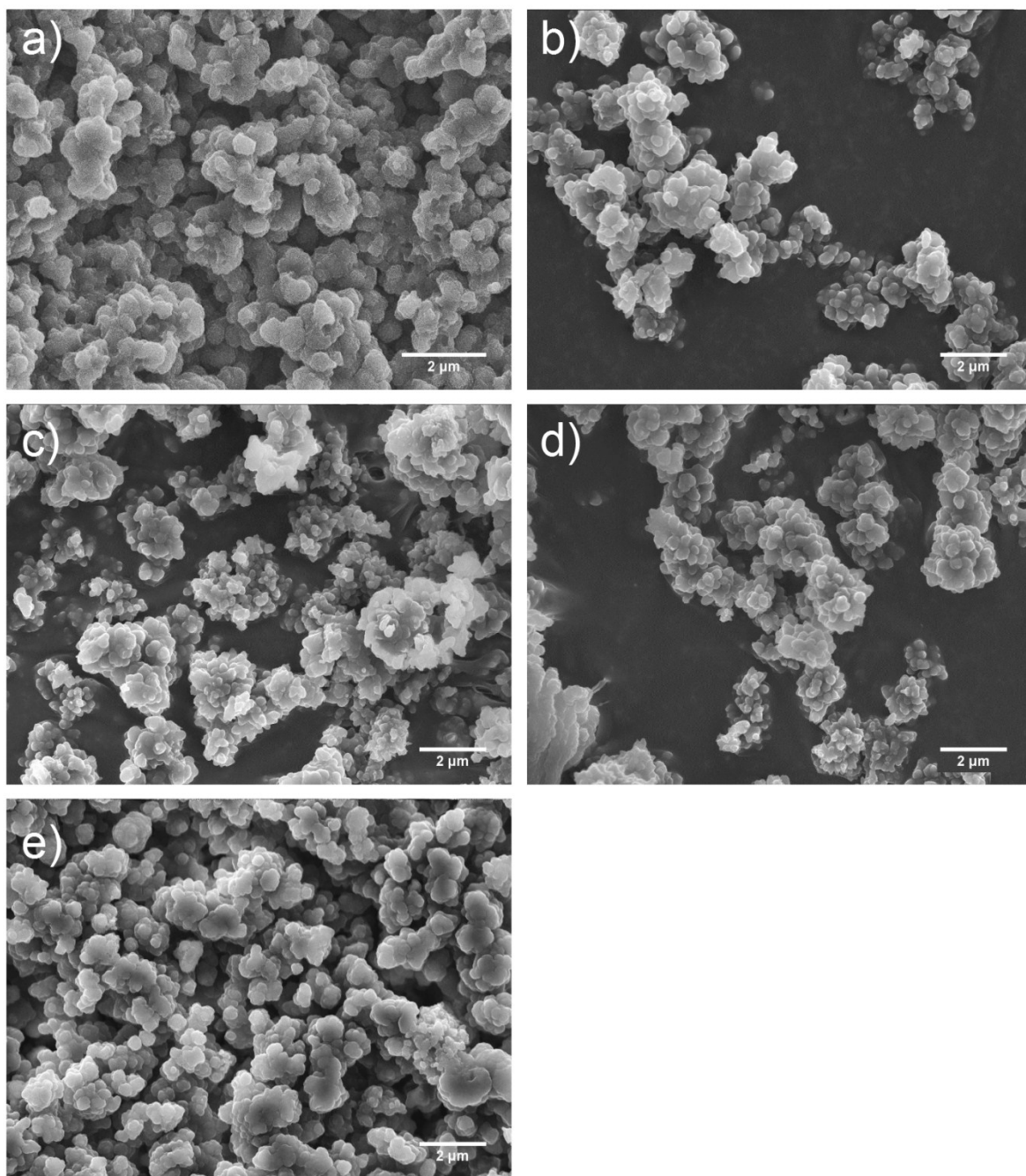


Figure S13. SEM micrographs of (a) BDT COF, (b) BDT:BDT-OEt 3:1 COF, (c) BDT:BDT-OEt 1:1 COF, (d) BDT:BDT-OEt 1:3 COF, (e) BDT-OEt COF, respectively.

Section 5. TEM micrographs

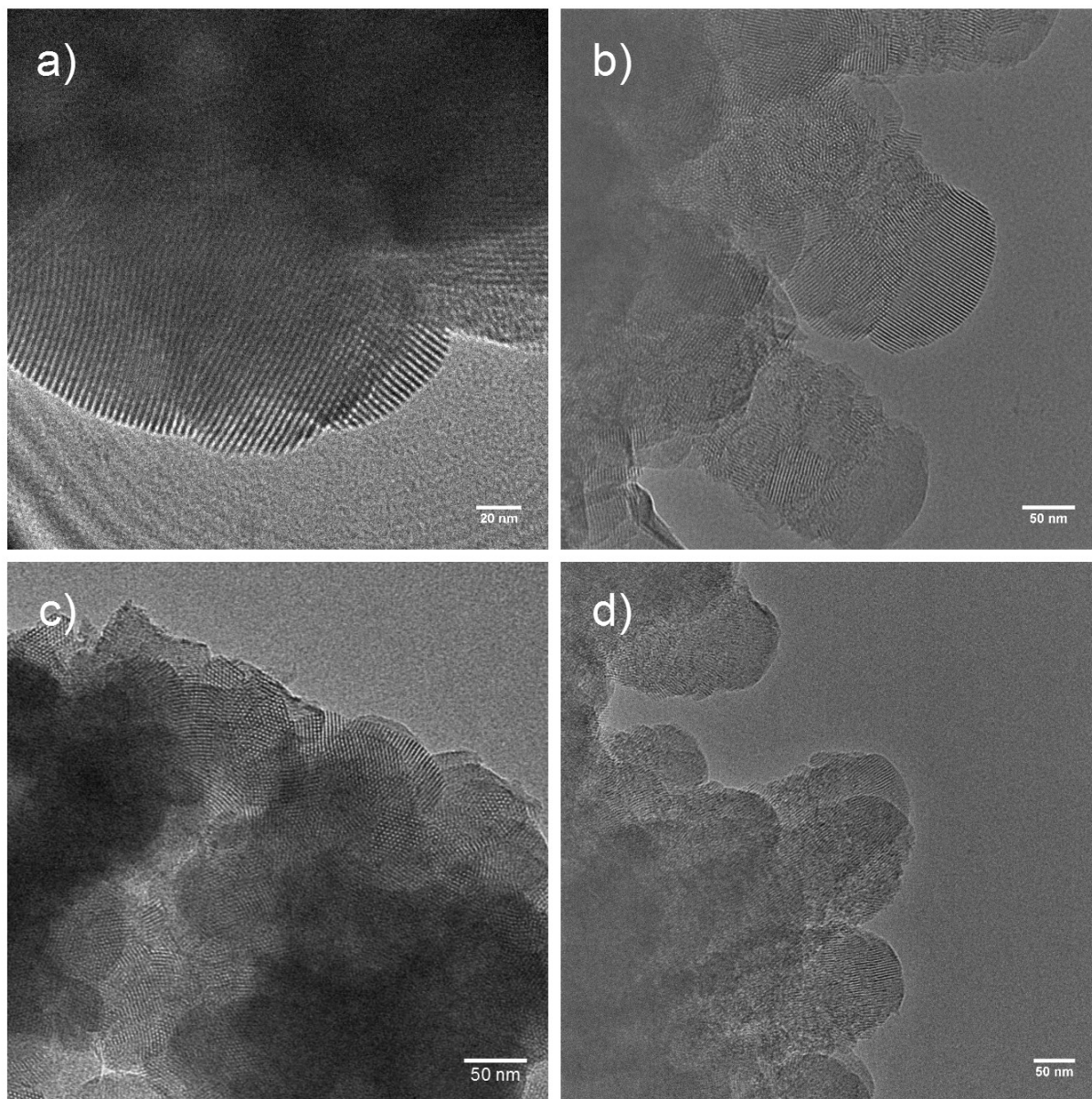


Figure S14. TEM micrographs of (a) BDT COF, (b) BDT:BDT-OEt 3:1 COF, (c) BDT:BDT-OEt 1:1 COF, (d) BDT:BDT-OEt 1:3 COF, respectively.

Section 6. Thermogravimetric analysis

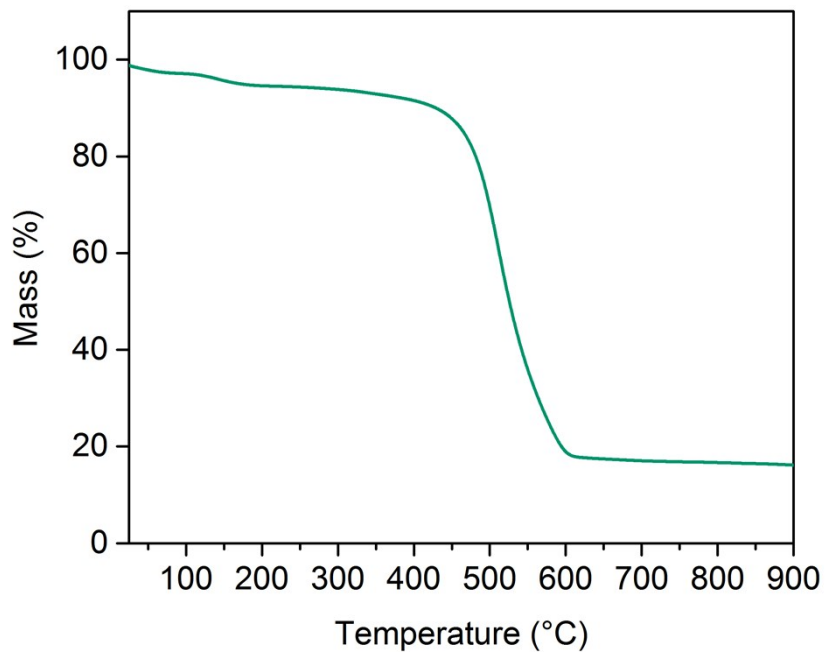


Figure S15. TGA trace of BDT COF.

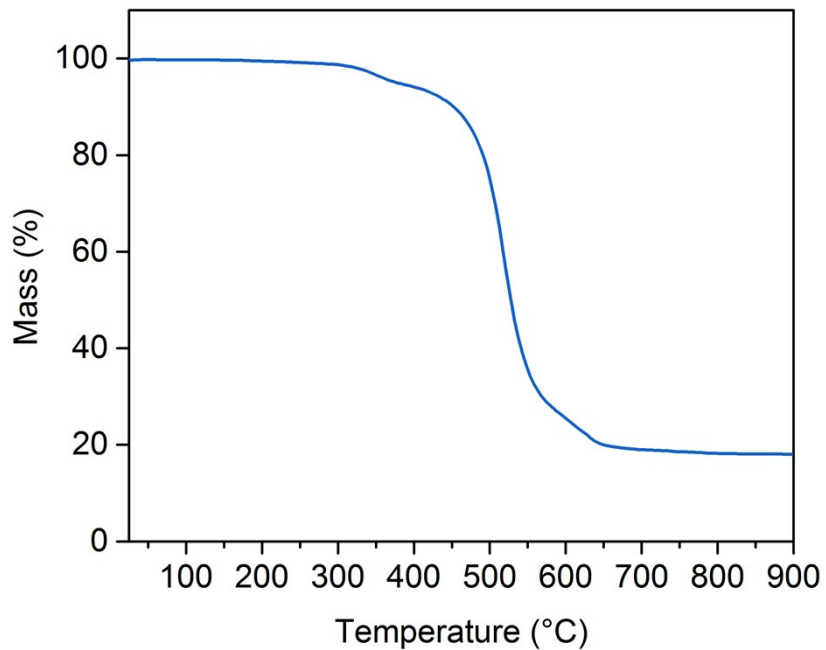


Figure S16. TGA trace of BDT:BDT-OEt 3:1 COF.

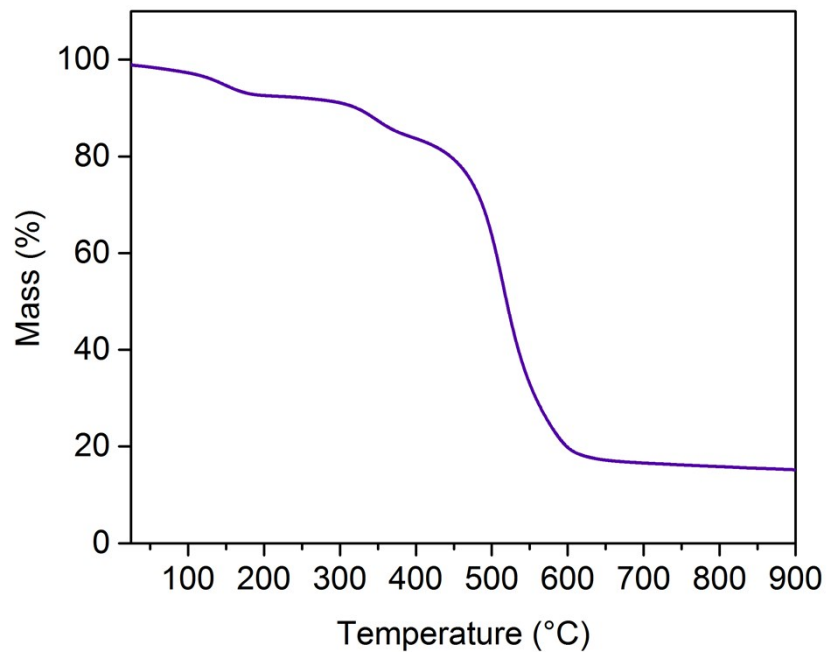


Figure S17. TGA trace of BDT:BDT-OEt 1:1 COF.

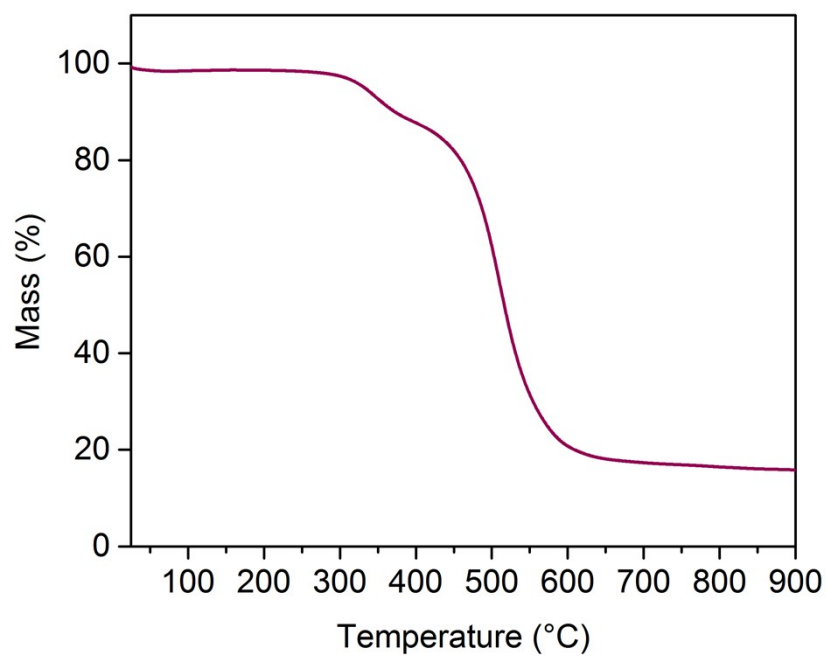


Figure S18. TGA trace of BDT:BDT-OEt 1:3 COF.

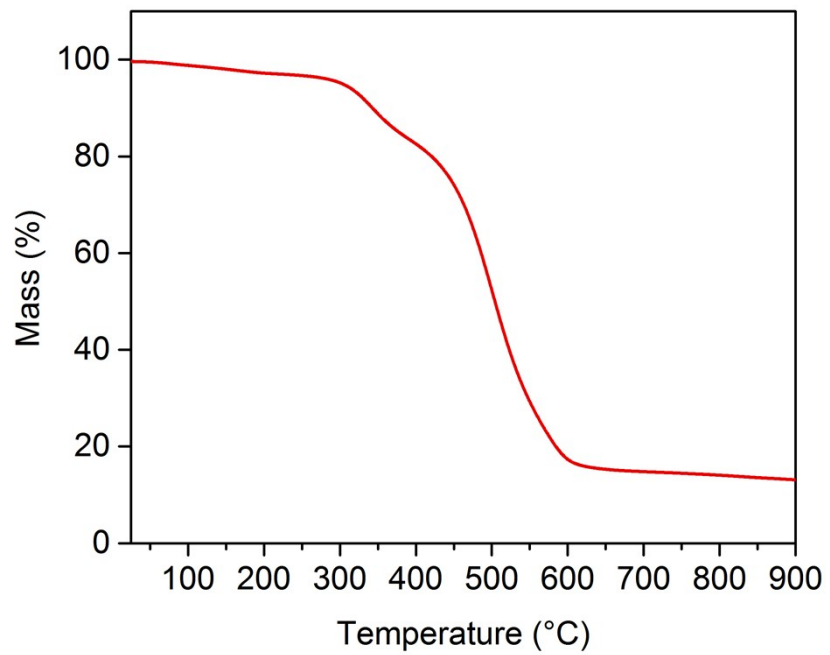


Figure S19. TGA trace of BDT-OEt COF.

Section 7. FT-IR spectra

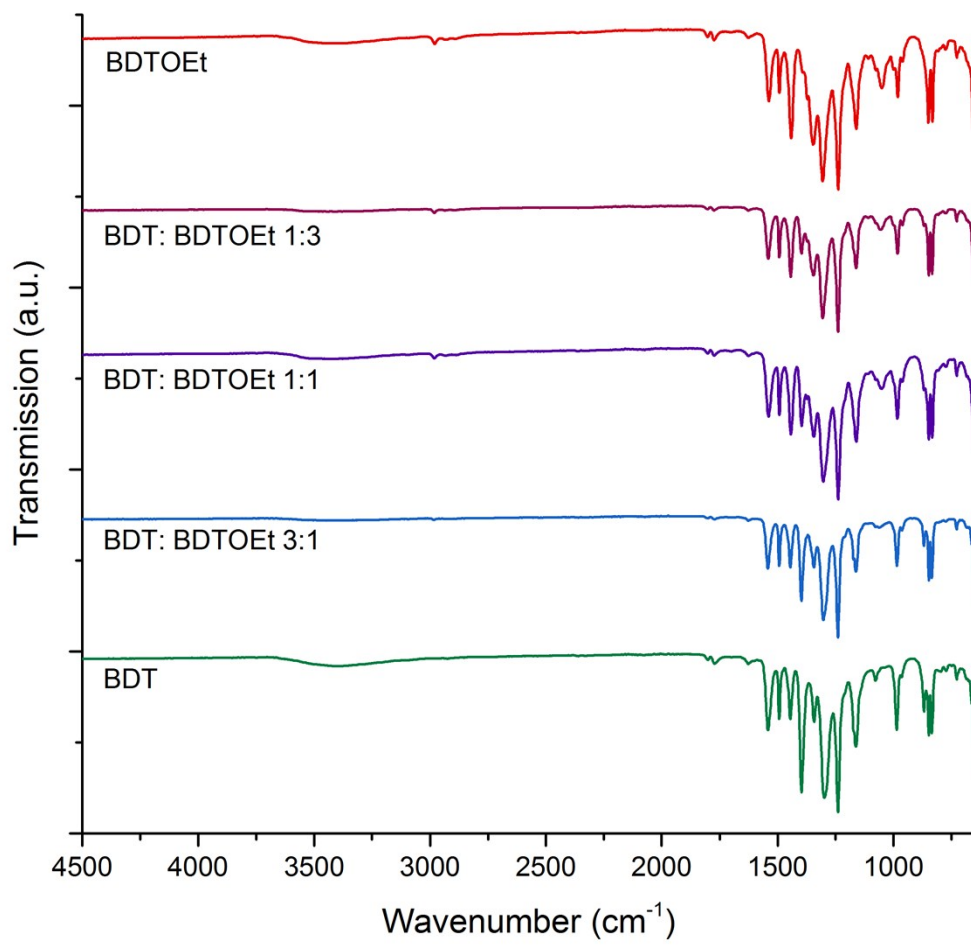


Figure S20. FT-IR plots of BDT COF, BDT:BDT-OEt COFs and BDT-OEt COF.

Section 8. PXRD small angle region

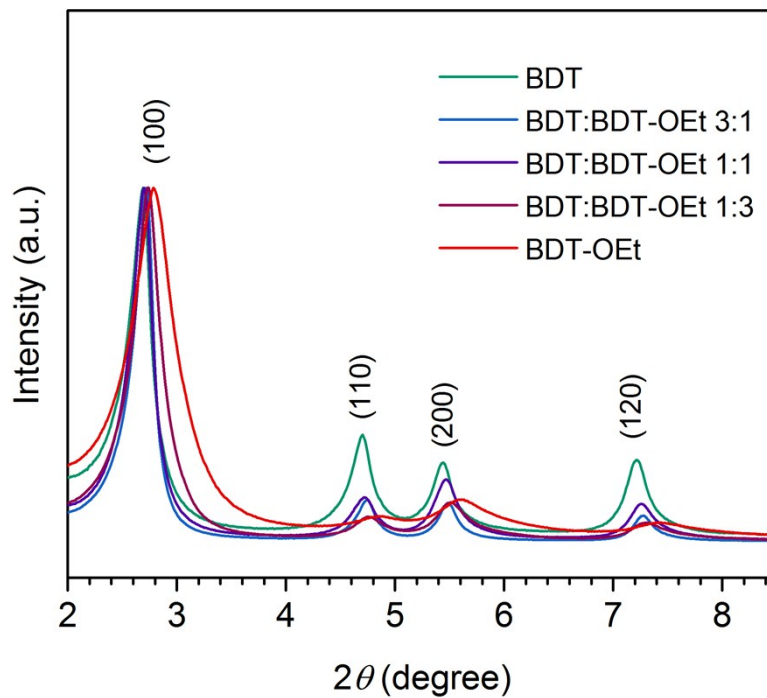


Figure S21. PXRD patterns of BDT COF, BDT:BDT-OEt COFs, and BDT-OEt COF: small angle region showing a gradual shift of the reflections corresponding to the ab plane to higher 2 theta values with the higher integrated fraction of BDT-OEt building units.

Section 9. Solid state NMR spectra of BDT-OEt COF

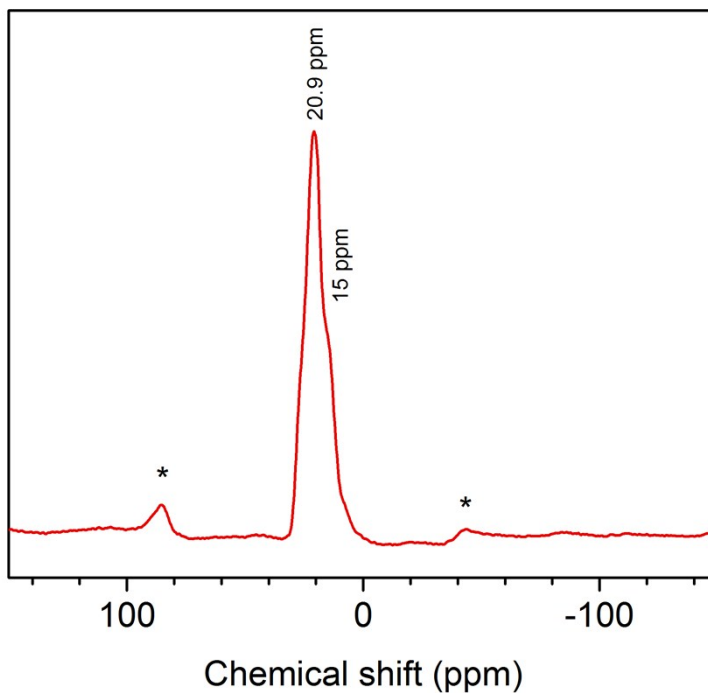


Figure S22. ^{11}B ssNMR spectrum of BDT-OEt COF showing a boronic ester peak at 20.9 ppm. The shoulder peak at 15 ppm is attributed to free boronic acid groups present as terminal moieties of the framework. Asterisks indicate spinning side bands.

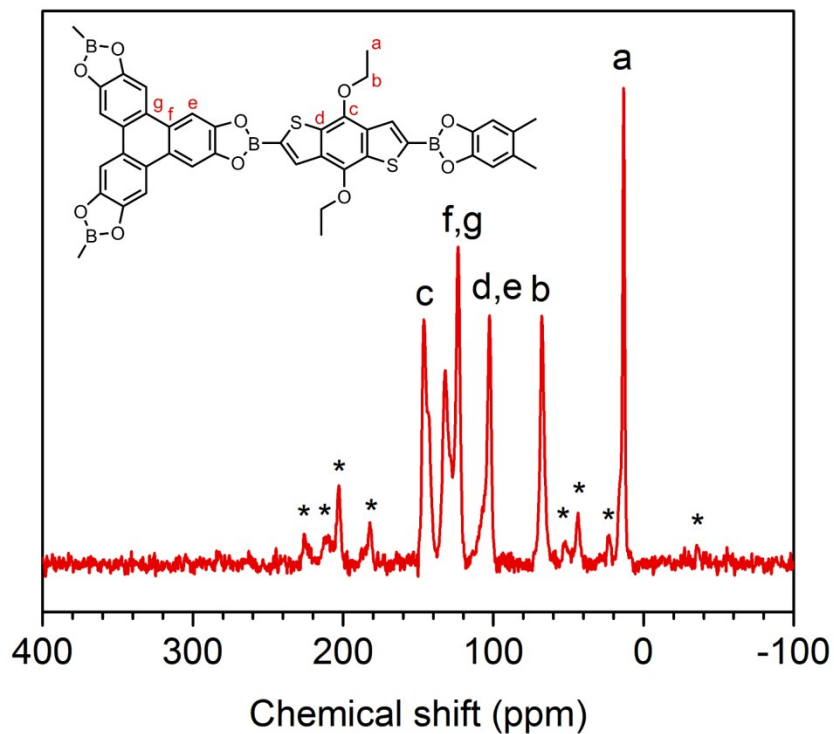
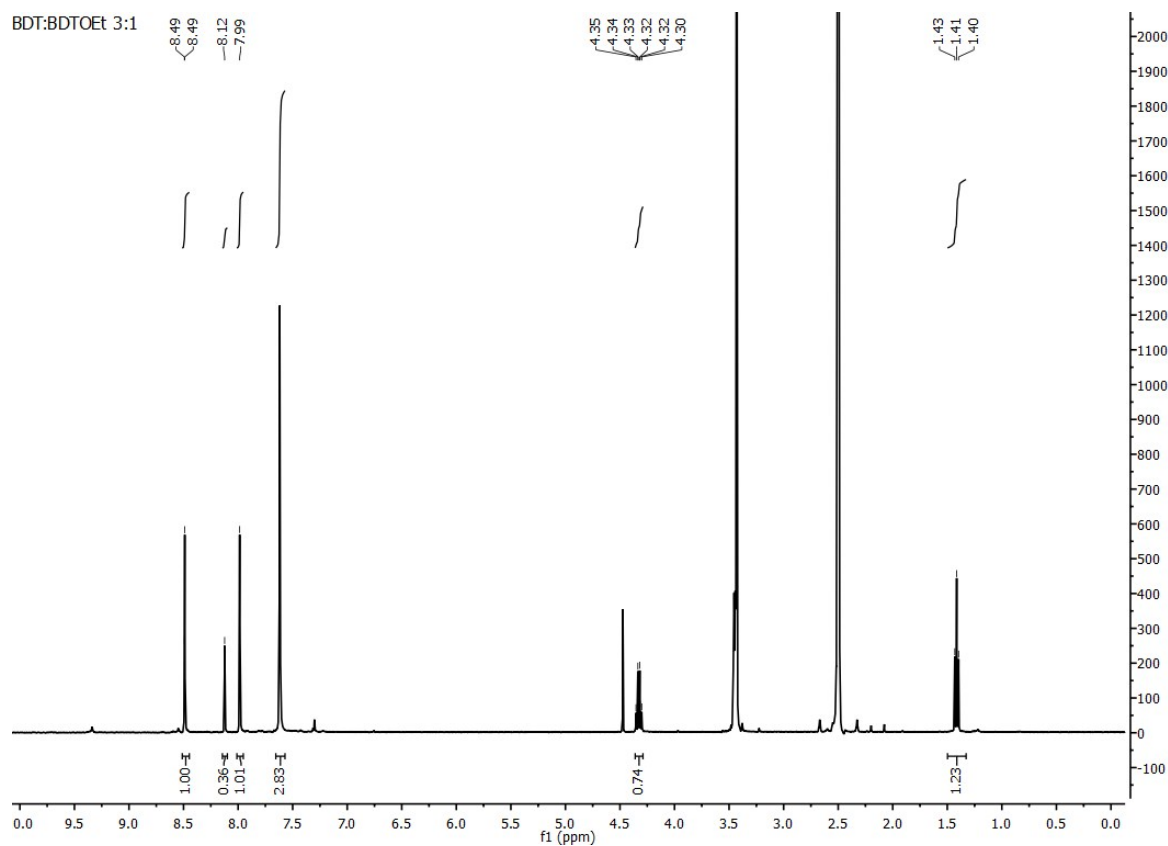
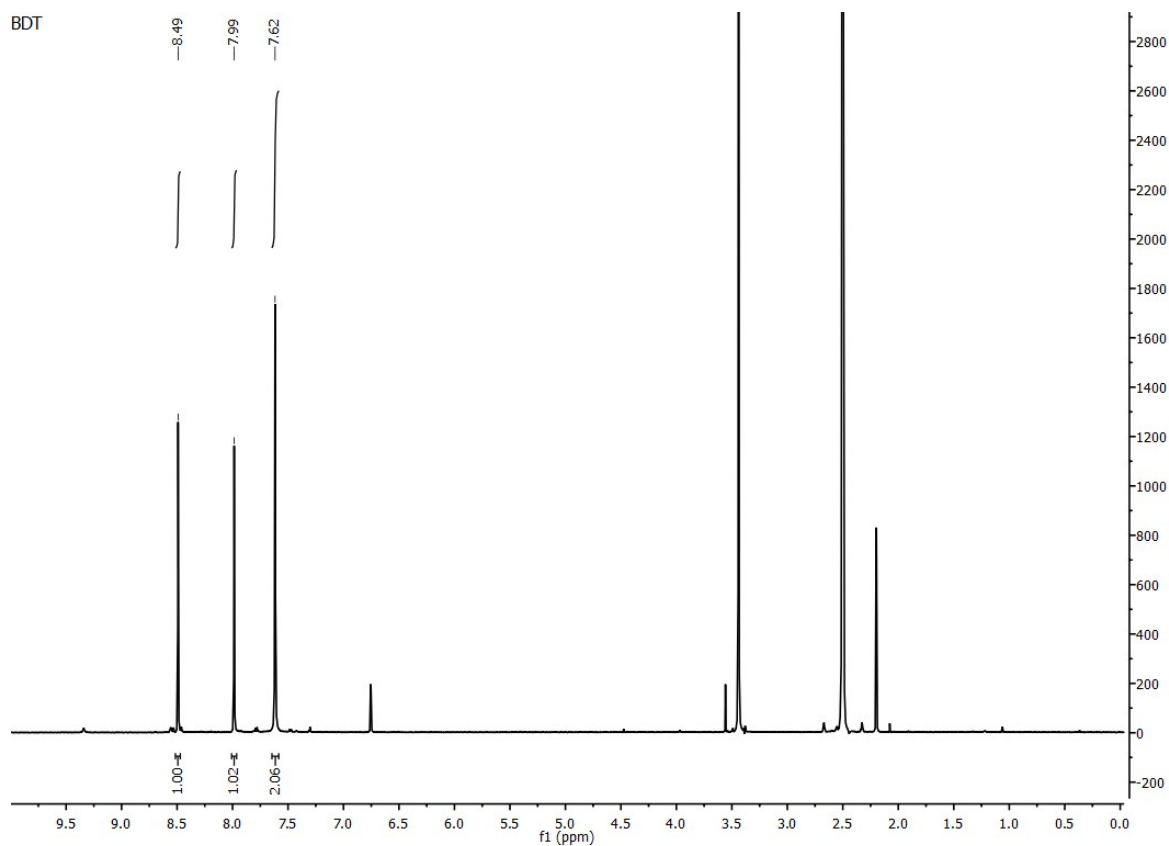
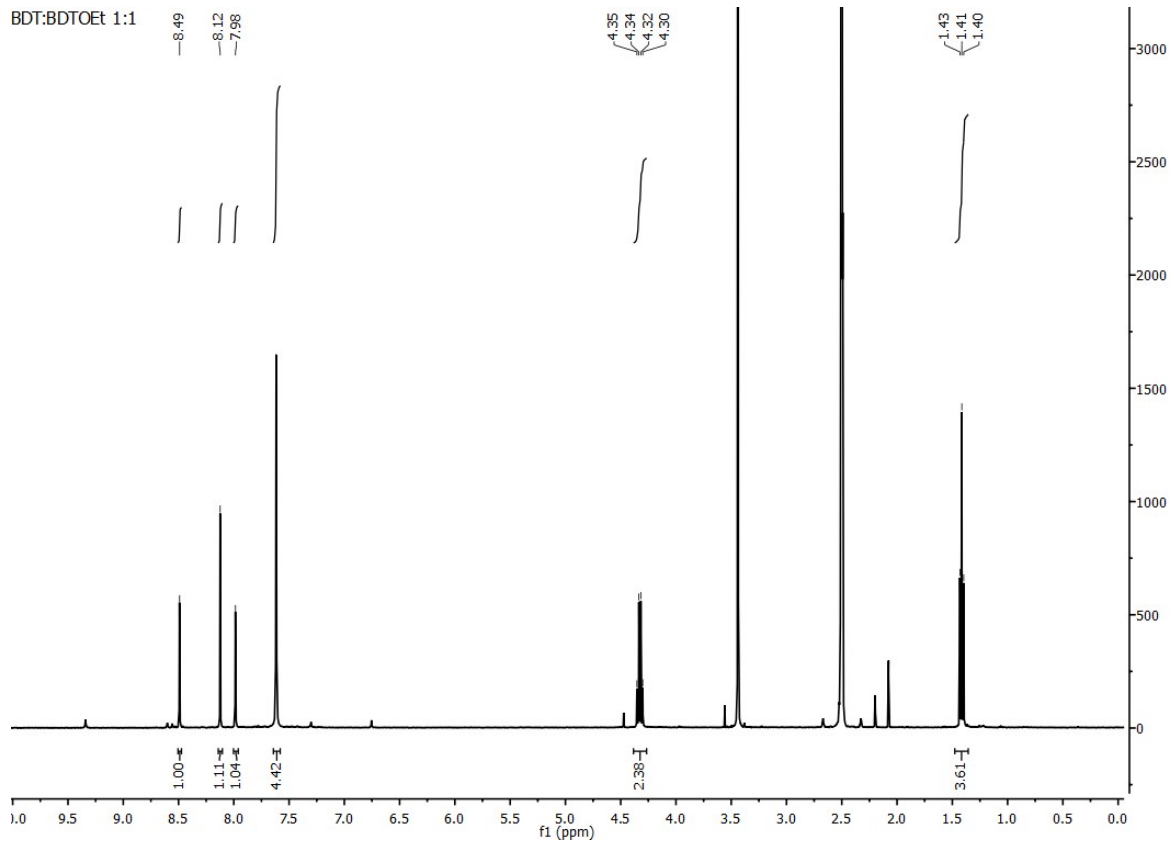


Figure S23. ^{13}C ssNMR spectrum of BDT-OEt COF. Asterisks indicate spinning side bands.

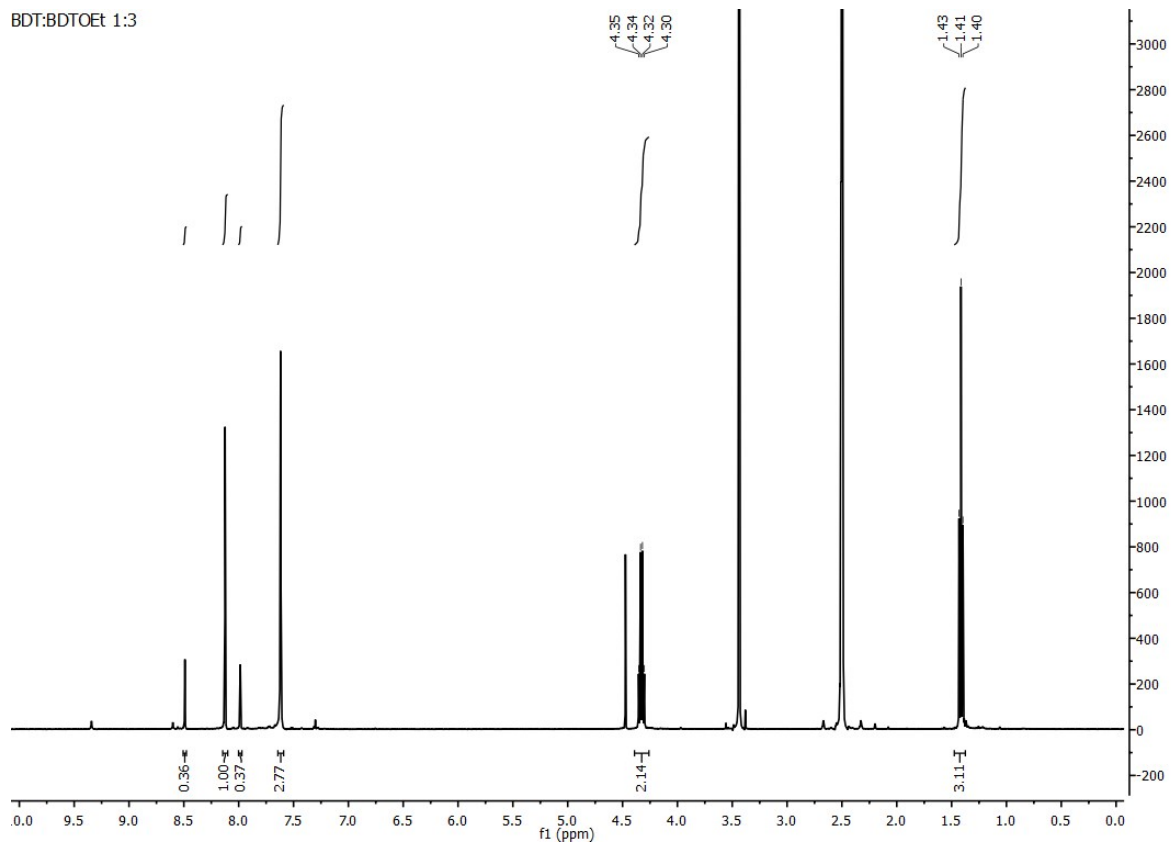
Section 10. NMR spectra of hydrolysed COFs



BDT:BDTOEt 1:1



BDT:BDTOEt 1:3



BDTOEt

